

Many-body theory of effective local potentials for electronic excitations. III. Application to giant dipole resonances

Željko Crljen*

Serip Physics Laboratory, Rutgers University, Piscataway, New Jersey 08854

Göran Wendin

Institute of Theoretical Physics, Chalmers University of Technology, S-41296 Göteborg, Sweden

(Received 5 June 1986)

The $4d \rightarrow f$ transitions in Xe and Ba and the $4p \rightarrow d$ transition in Kr are analyzed in terms of the effective wave functions and effective local potentials in an energy region where the response of the system is highly resonant and shows collective behavior. The effective potentials are obtained in the random-phase approximation with exchange, and the importance of relaxation is investigated. It is found that the energy dependence of the effective potential is necessary to describe the excitation spectrum reasonably well. The effects of external screening by adding and removing electrons (Ba^{1-} - Ba^{2+}) are analyzed and the applicability of the atomiclike model for the $4d \rightarrow f$ transitions in metallic Ba is discussed.

I. INTRODUCTION

The calculation of accurate photoionization cross sections for atoms provides a good test of our understanding of atomic structure and dynamics. The effective transition amplitude for photoionization, accounting for the important many-body effects (polarization, core relaxation), can be obtained through an effective wave function for the excited state, as shown in the two previous papers^{1,2} in this series (hereafter referred to as I and II). From this effective wave function one can construct a corresponding local potential which makes it straightforward to understand the dynamics of the one-electron excitation processes.

Photoionization of Xe and surrounding elements ($Z=46-70$) in the region of the $4d \rightarrow f$ excitations has been extensively studied during the last twenty years (see, e.g., Refs. 3-10 and references therein). The $4d$ excitation spectra of the elements from, say, Xe to Sm are characterized by a giant dipole resonance structure¹⁰⁻¹⁴ which peaks in the region above the $4d$ ionization threshold and shows very weak absorption lines in the discrete energy region. There have been a number of calculations employing different approaches and approximations. The existence of a shape resonance in Xe was already shown by Cooper¹⁵ using a Hartree-Fock potential and by Manson and Cooper¹⁶ using a Herman-Skillman potential. Subsequently, RPAE (random-phase approximation with exchange) calculations were very successful in describing the observed spectra in the $4d$ absorption region of Xe,¹⁷⁻¹⁹ showing that the collective response of the $4d$ shell governs the excitation. Furthermore, with inclusion of core relaxation effects, the RPAE calculations reproduced the general features of the $4d$ photoionization spectra of Ba and La.^{13,20-23} Recently some other approaches, such as the time-dependent local-density approximation^{24,25} (TDLDA) and the local-density-based random-phase approximation^{10,26} (LDRPA) also have

shown to be very successful in calculations of the photoionization cross section in the $4d$ energy region of Xe and Ba (see I and II for further discussion).

The distribution of oscillator strength in the $4d$ absorption region of the elements mentioned above, can be qualitatively understood in terms of the effective local potential for the excited f states. Generally speaking, the potential for the excited state, has a two-well structure.^{14,15,27-33} For instance, in atomic Xe with a $4d$ hole, at low kinetic energies the f electrons are kept away from the inner well by positive potential barrier, giving a very small overlap with the $4d$ wave function. At higher kinetic energies, the f orbital penetrates into the inner region of the potential increasing the overlap with the core wave function. This leads to an increase in oscillator strength (delayed onset⁴) and to a resonance structure in the cross section.

The shape of the one-electron potential is of critical importance for the behavior of the photoionization cross section. The original calculations^{15,16} were based on Hartree-Fock average-of-configuration (HF_{av}) or Hartree-Fock-Slater (Herman-Skillman) potentials, which represent ground-state potentials.^{1,2} Wendin and Starace²⁷ derived potentials for excited states ($4d \rightarrow 4f, 5f$ in Ba and La) in the LS -dependent Hartree-Fock picture (HFLS), and showed the connection between the HF_{av} and the $\text{HF } ^1P$ potentials and wave functions in terms of the response to electron-hole excitations. Crljen and Wendin subsequently extended this work by treating the excitations within the RPAE, by considering continuum excitations, and by investigating other systems and transitions (preliminary results were reported in Ref. 34). Among other things, it was found that in the HFLS and RPAE schemes, the effective one-electron potential may show an important energy dependence in the resonance region. The depth of the inner well as well as the height of the barrier can be subject to changes, leading to changes in the overlap and consequently in the transition amplitude.

Wendin *et al.*^{27,34} only considered the frozen-core approximation. However, relaxation effects were known to be very important for Ba and La (Refs. 12, 13, 20–23) (and for the first part of the lanthanide series), and effects of statically relaxed ion cores were incorporated within the HF 1P and RPAE schemes in subsequent work.^{1,35} Also, Griffin and Pindzola³¹ have studied the energy dependence of the effective f potential for $4d \rightarrow \epsilon f$ HF 1P transitions in Ba (and $4d \rightarrow 4f$ HF 1P transitions in Sb^{3+} and Xe^{6+}) with inclusion of relaxation effects. As a result of core relaxation, the inner-well region of the effective potential is shifted upwards^{1,31} (less attractive potential), resulting in a strongly enhanced “collective” barrier and a delayed onset of the photoionization cross section. A general discussion of the effective excitation potential in various approaches and approximations has been given in papers I and II (Refs. 1 and 2).

In this paper we first recapitulate the basic formulas for calculating the effective wave function and the effective potential for the excited state in HF and RPAE approximations.

We then present the analysis of the electronic excitation potential in the $4p \rightarrow d$ excitation process in Kr, showing an energy dependence of the potential over a wide energy range in the HF_{av} , HF 1P and RPAE approximations. The energy dependence is of particular importance for comparison with the semiempirical three-parameter energy-independent potential of Miller *et al.*^{36,37} We demonstrate that a degree of energy dependence is necessary in order to give a good description of the photoionization cross section.

We also analyze the $4d \rightarrow f$ excitations in Xe and compare the RPAE effective potential with the effective potential from an LDRPA type of approach.

Finally, we focus attention on $4d \rightarrow f$ excitations in Ba in different stages of ionization. We show that with increasing ionicity (in going from Ba to Ba^{1+} and Ba^{2+}), the inner well of the effective potential for the f electron (calculated within the RPAE with a relaxed $4d$ hole) is almost rigidly moving down while retaining its shape. The effect on the photoionization cross section is that the overall width of the spectral distribution does not change, although the ionization threshold moves to higher energies. We shall also comment on the applicability of the atomiclike model for the $4d \rightarrow f$ excitation in metallic Ba.

II. EFFECTIVE WAVE FUNCTIONS AND CORRESPONDING EFFECTIVE LOCAL POTENTIALS

We base our calculation of the effective wave functions and the corresponding local potentials on a diagrammatic and response function analysis of the atomic polarizability as presented in I and II. A zeroth-order approximation is defined in terms of single-particle-hole excitations in a frozen environment, and we let the perturbation expansion account explicitly for polarization and core-relaxation effects. The definition of the zeroth-order approximation leads us to use Hartree-Fock wave functions for occupied (hole) states and to calculate the excited (particle) states using the HF V^{N-1} potential.³⁸ There are typically two

cases of the HF V^{N-1} potential, namely, the HF_{av} V^{N-1} (configuration average potential) and the HFLS (LS -dependent HF) V^{N-1} potential. The wave functions in the HF_{av} V^{N-1} potential and the HFLS V^{N-1} potential are obtained from the Hartree-Fock equations of the form^{1,2}

$$\left[-\frac{d^2}{dr^2} + \frac{l(l+1)}{r^2} - \frac{2Z}{r} + V_H(r) - \epsilon_i \right] u_i(r) = X_i(r) \quad (2.1)$$

using the appropriate coefficients in the exchange $X_i(r)$ term.^{15,38} In Eq. (2.1), $V_H(r)$ is the Hartree electrostatic potential from the electronic charge distribution; r is expressed in atomic units and energies and potentials in rydbergs. The wave functions obey the usual normalization conditions for atomic orbitals, discrete and continuum, respectively,

$$\int_0^\infty u_i^2(r) dr = 1, \quad (2.2a)$$

$$\int_0^\infty u_\epsilon^2(r) dr = \delta(\epsilon - \epsilon'). \quad (2.2b)$$

A local potential giving the wave function in Eq. (2.1) can be obtained easily by the relation^{1,27,39}

$$V_i(r) = -\frac{2Z}{r} + V_H(r) - \frac{X_i(r)}{u_i(r)}, \quad (2.3)$$

since the quantities $V_H(r)$ and $X_i(r)$ are available directly in a HF program. With the help of Eq. (2.3) we can analyze the contribution of the exchange term to the local potential. The effective wave function $u_i^{\text{eff}}(r)$ for an excited state in a single-channel excitation process, including many-body effects within the RPAE as well as relaxation effects are calculated as described in II, Sec. IV [Eq. (4.19)]. The effective wave functions are available in numerical form. We find the corresponding effective local potential by using the relations^{1,2,40}

$$V_i^{\text{eff}}(r) = \left[\left[\frac{d^2}{dr^2} + \epsilon_i \right] u_i^{\text{eff}}(r) \right] / u_i^{\text{eff}}(r), \quad (2.4)$$

$$V_i^{\text{eff}}(r) = V_i(r) + \frac{l(l+1)}{r^2}. \quad (2.5)$$

These relations are also used to obtain the effective potential in the LDRPA. The potential $V_i(r)$ is singular at the nodes of the wave function. The singularity is characteristic of a particular wave function and energy.

As discussed in II, representation of the RPAE in terms of an effective one-electron wave function and potential introduces an operator dependence: The dipole-length and dipole-velocity formulations will lead to different effective wave functions and potentials because *ground-state (initial-state) correlations* enter in different ways (opposite sign). In this paper we shall only present RPAE results based on the dipole-length formulation (RPAE- L).

III. APPLICATION TO EXCITATIONS IN Kr, Xe, AND Ba

We shall discuss the results of numerical calculations of the $4d \rightarrow f$ ionization of atomic Ba and Xe and the $4p \rightarrow d$

ionization of atomic Kr at different levels of approximation. The starting point will be the frozen core HF V^{N-1} average-of-configuration potential (HF_{av}) (Ref. 38) which describes the electron-hole excitation as decoupled from the rest of the system. Subsequently, a coupling of the electron-hole excitation to a 1P angular momentum state will be considered. The result can be obtained from an HF 1P calculation or equivalently from the Tamm-Dancoff approximation with exchange (TDAE) many-body scheme.¹³ Inclusion of Fermi-sea correlation leads to the well-known RPAE scheme which has been very successful in describing the gross distribution of the oscillator strength in strongly interacting regimes. Nevertheless, in many cases relaxation effects are important or at least significant. The effect of relaxation is twofold:^{1,12,13,20} It lowers the ionization threshold and broadens the ionization cross section. Here we only take into account static monopole relaxation by using a relaxed ionic potential for excited states. We have used the ΔSCF method^{41,42} (change in self-consistent field Hartree-Fock and Dirac-Fock) to obtain relaxed hole energies.

We shall also present results (effective one-electron wave functions and potentials) obtained using a local-density based random-phase approximation (LDRPA).^{10,26} In comparison with the RPAE, the LDRPA provides a very simple method for obtaining quite accurate photoionization cross sections of atomic subshells including intershell coupling.

A. Kr

We have analyzed $4p \rightarrow d$ excitations in atomic Kr, a case which has been studied by many workers.^{4,16,17,37,43,44} Figure 1 shows photoabsorption cross sections obtained in different approaches and approximations. It is clear that these excitations involve many-electron polarization effects, since one-electron schemes such as $X\alpha$, LDA and HF_{av} fail to describe the overall shape of the cross section, placing the bulk of the oscillator strength at too low ener-

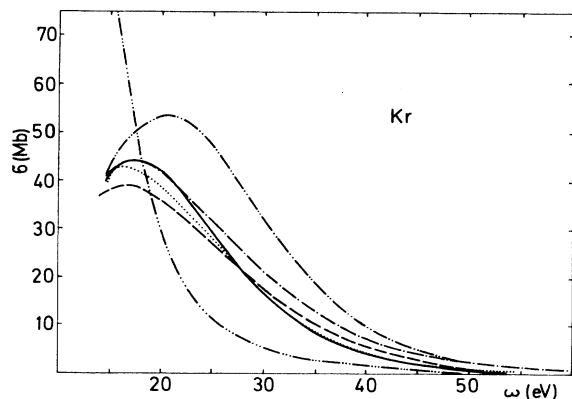


FIG. 1. Kr $4p$ photoionization cross sections; (\cdots) experimental measurement of Marr and West (Ref. 45); (---) RPAE result, frozen $4p$ hole; (---) RPAE result with relaxed $4p$ hole; ($\text{-}\cdot\cdot\cdot\text{-}$) HF^1P (length) and ($\text{-}\cdot\cdot\cdot\text{-}$) HF_{av} result with frozen $4p$ hole; ($\text{-}\cdot\cdot\text{-}$) pseudopotential analysis of Miller *et al.* (Ref. 37) (average length-velocity dipole operator).

gies. With inclusion of the dipole polarizability of the $4p$ subshell through the HF 1P potential, the oscillator strength is shifted to higher energies. Adding Fermi-sea correlations, which leads to the RPAE, causes redistribution of the oscillator strength and provides very good agreement with experimental results. The effective local potentials for continuum d levels in different approaches and approximations, are plotted in Fig. 2 (continuum energy $\epsilon=0.1$ Ry). As seen in the figure, the weakly attractive potential in the HF_{av} scheme becomes strongly repulsive in the HF 1P scheme. The narrowing of the inner well, and the barrier in the effective potential are due to the interaction of the electron-hole excitation with the remaining electrons in the $4p$ subshell, i.e., it is a consequence of induced many-electron polarization effects. To emphasize this feature, the barrier was characterized as a collective barrier.³⁴ Such barriers also exist in $3p$ excitation of Ar and $5p$ and $4d$ excitations in Xe, Ba, and La, to mention only a few examples (see, e.g., Refs. 1, 27, 31, and 34).

A consequence of the collective (polarization) barrier in the HF 1P potential at low kinetic energies, shown in Fig. 2, is to prevent the electron wave function from entering into the inner region, which makes the oscillator strength in HF 1P smaller in comparison with the oscillator strength in HF_{av} at a given, low, kinetic energy ($\epsilon=0.1$ Ry). The barrier is even more pronounced when Fermi-sea correlations are taken into account through the RPAE, giving even smaller oscillator strength. These considerations depend, of course, on the energy chosen.

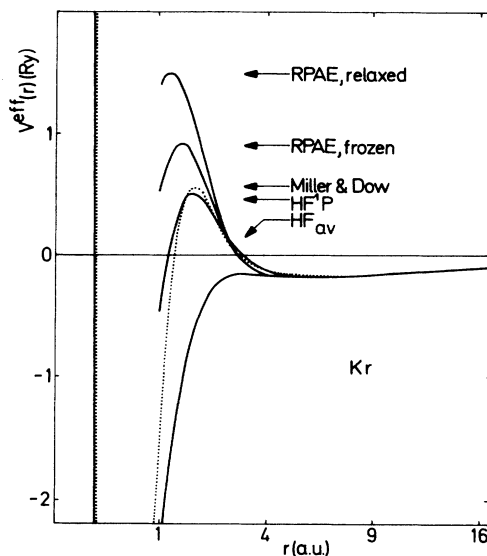


FIG. 2. Effective one-electron potential for Kr ($4p\epsilon d$), energy of excited state $\epsilon=0.1$ Ry. In the barrier region of the effective potentials calculated in HF 1P and RPAE, there are singularities at $r\sim 0.77$ a.u. (at the position of the nodes of effective wave functions) which are not drawn. Minima of the potential wells, at $r=0.21$ a.u. are -34.53 Ry, in HF_{av} approximation; -34.40 Ry in HF 1P ; -34.26 in RPAE, frozen $4p$ hole; -33.86 Ry in RPAE, relaxed $4p$ hole. The figure also shows the energy-independent local parametrized potential of Miller *et al.* (Ref. 37) which has a minimum of -44.28 Ry at $r=0.205$ a.u.

In the HF_{av} approximation the effective potential is almost energy independent and at higher energy ($\epsilon=1$ Ry, for example), the HF_{av} wave function enters deeply into the inner region and, because of rapid oscillations, it produces a smaller overlap with the $4p$ wave function and consequently smaller cross section than for lower energy (at $\epsilon=0.1$ Ry). At an energy of 1 Ry, it produces a smaller overlap with the $4p$ wave function than that produced by the $\text{HF } ^1P$ and RPAE wave functions, which are kept further out by the barrier.

As seen in Fig. 3, the barrier in the (RPAE-length) effective local potential decreases with increasing kinetic energy. The most rapid decrease of the barrier occurs for kinetic energies in the range from threshold to just above the cross section maximum, i.e., before the wave function has fully penetrated the barrier. At sufficiently high kinetic energies, the RPAE collective (polarization) contribution represents a small perturbation of the HF_{av} potential for independent electron excitations, and consequently the oscillator strengths and cross sections become closely similar. However, there are some important distinctions to be made regarding the high-energy behavior of the RPAE length and the $\text{HF } ^1P$ one-electron potentials.^{2,46} In the $\text{HF } ^1P$ scheme the polarization contribution decreases only very slowly, connected with the reduced electron-hole overlap and the decrease of the exchange integral. In the RPAE, however, the interference between initial- and final-state effects leads to an explicit dependence on the excitation (photon) energy (ω^{-1}). As a consequence, the collective barrier decreases more rapidly in the RPAE than in the $\text{HF } ^1P$ approach. This is an essential feature of the RPAE which gives sum-rule conserving cross sections and good agreement with experiment.

With this analysis we can understand the differences

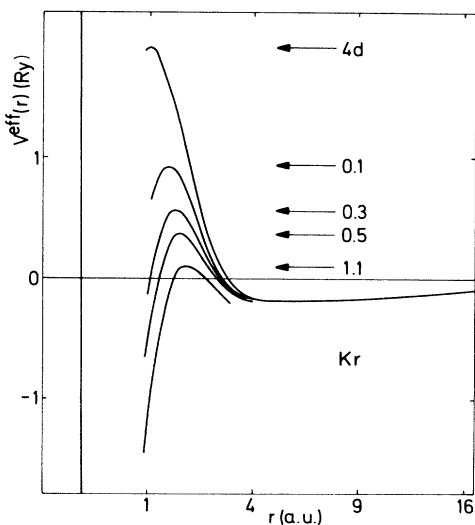


FIG. 3. Energy dependence of the ($4p4d, \epsilon d$) RPAE-length local effective potential, frozen $4p$ hole, for atomic Kr. The singularities at the position of the nodes of the wave functions $r \sim 0.77$ a.u. are not drawn.

between the photoionization cross sections in the HF_{av} , $\text{HF } ^1P$ and RPAE schemes at various kinetic energies, and draw conclusions about the importance of collective effects (polarization; electron-hole “exchange”). For instance, we find that exchange effects are more important at energies close to the ionization threshold and in the discrete region than at higher energies. In particular, in the threshold region, weakly penetrating orbitals and a strongly delayed onset does not mean that exchange effects (collective effects) are weak. On the contrary, the change in going from HF_{av} to $\text{HF } ^1P$ or RPAE may be enormous. This means that the coupling schemes for discrete levels must take into account exchange effects within the $\text{HF } ^1P$ or RPAE even if the discrete spectrum is very weak due to a delayed onset type of cross section (a nice example being the $4d \rightarrow nf$ excitations in Ba).

In Fig. 2 we have plotted the RPAE effective potential obtained with the relaxed $4p$ hole [binding energy $|\epsilon_{4p}| = 0.98$ Ry; HF binding energy for an unrelaxed $4p$ hole $|\epsilon_{4p}| = 1.05$ Ry]. It is evident that the screening charge is pulled into the inner region with respect to the frozen RPAE potential, which raises the inner-well and barrier regions of the entire potential relative to the vacuum (or the fixed bottom of the outer Coulomb well). The consequence is that the RPAE with relaxation of the $4p$ hole will broaden the ionization cross section in comparison with the RPAE without relaxation effects. However, the agreement with experiment is now worse. Inclusion of correlation effects may change this. The $4p$ binding energy will be effectively pushed back up. The effect on the potential has not been investigated but it should make the potential more attractive. This would tend to compensate the effect of relaxation.

In the light of the work of Miller *et al.*^{36,37} on a semiempirical three-parameter potential, the question of the energy dependence of a potential is an interesting subject. The semiempirical energy independent potential^{36,37} was determined to reproduce the average energy dependence of the β parameter in the angle-resolved photoionization cross section for kinetic energies in the 0–6 Ry range. It therefore represents an excited state potential, different from the ground state potential used for calculation of the $4p$ orbital. As seen in Fig. 2 the potential Miller *et al.*³⁷ obtained is close to a $\text{HF } ^1P$ potential for low kinetic energy ($\epsilon=0.1$ Ry). On the ground that it would lead to better fulfillment of the oscillator strength sum rule they used the average of the dipole-length and dipole-velocity operators in calculation of the photoabsorption cross section. As demonstrated in II, this will give a cross section reasonably close to the RPAE cross section, if combined with the $\text{HF } ^1P$ effective one-electron wave function. The drastic lowering of the potential barrier with increasing kinetic energy in the RPAE, as shown in Fig. 3, explains why their photoabsorption cross section is too high in the region 0.5–3 Ry above the threshold. The high static barrier keeps the electron wave function out, resulting in less cancellation in the $4p$ region. The consequence is then that in this energy range a high static barrier produces a larger cross section than a lower barrier. A degree of energy dependence of the parametrized potential is therefore necessary to obtain a cross section in

better agreement with experiment. One could even get a parametrized energy-dependent potential from the first principle calculation, starting from the RPAE or HF 1P approximation. However, to obtain an analytic form of the effective potential one has to take care of the singularities which are characteristic of specific energies giving the right wave function and cross section.

B. Xe

The $4d \rightarrow f$ excitations in atomic Xe has been studied by many authors in different approaches and approximations.^{17-19,24,44} Figure 4 shows partial $4d \rightarrow f$ photoionization cross sections obtained in different approximations. The HF_{av} approximation places the bulk of the oscillator strength at too low energy. The HF 1P approximation results in shifting the oscillator strength to higher energy in comparison with the HF_{av} approximation. The reason for that is a prominent collective barrier which appears in the HF 1P potential at $r=1$ a.u., as seen in Fig. 5(a) for a kinetic energy of 2 Ry of the f electron. In a many-body language this barrier is a consequence of the strong polarization induced by the electron-hole excitation in the $4d$ subshell. In Fig. 5(a) is plotted the RPAE effective potential for the kinetic energy $\epsilon=2$ Ry, too. In order to describe the changes in the effective potential over this wide energy range (Fig. 4) we have to divide it into two regions: the first region extends from threshold to the cross section maximum, $\epsilon_m \approx 2$ Ry, and the other region extends from ϵ_m upwards. In the former region, going from HF 1P to RPAE results in small changes in the barrier (keeping almost the same area of the barrier) and consequently small changes in the oscillator strength. In the region of energies higher than ϵ_m , the oscillator strength is smaller in the RPAE than in the HF 1P . This is because the barrier (i.e., the area of the barrier, which actually determines the behavior of the wave function) is lower in the RPAE than in the HF 1P , as seen in Fig. 6. The

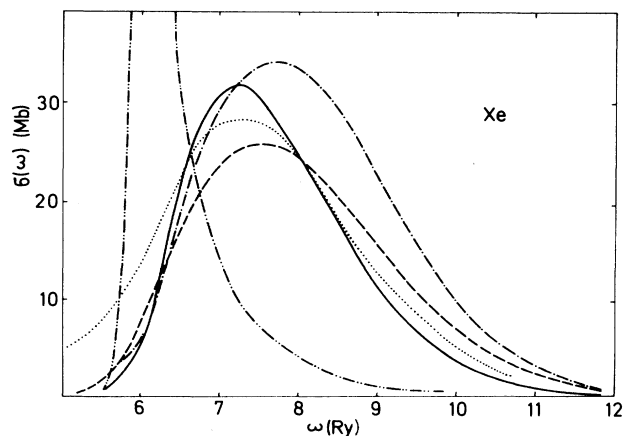


FIG. 4. $4d \rightarrow \epsilon f$ photoionization cross section for atomic Xe: (—) RPAE frozen $4d$ hole; (---) RPAE relaxed $4d$ hole; (-·-) HF 1P and (-·-·) HF_{av} on frozen $4d$ hole; (···) total photoionization cross section, experimental result of Haensel *et al.* (Ref. 47).

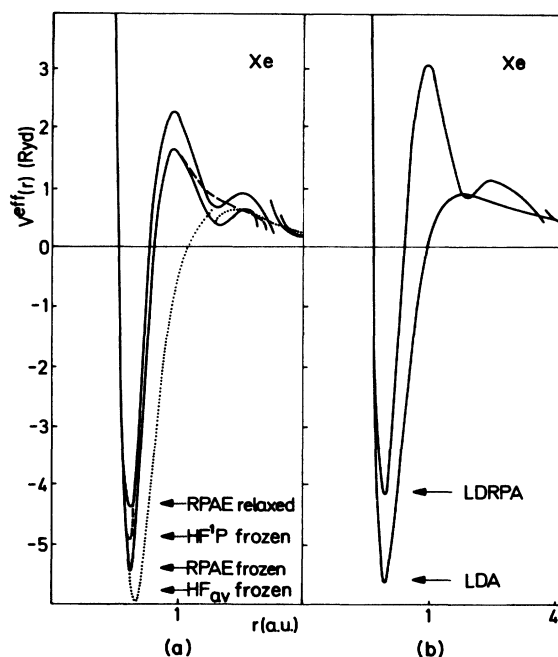


FIG. 5. Effective one-electron local potential for atomic Xe ($4d \rightarrow \epsilon f$), energy of excited f state $\epsilon=2$ Ry, at $\sigma \sim \sigma_{\max}$.

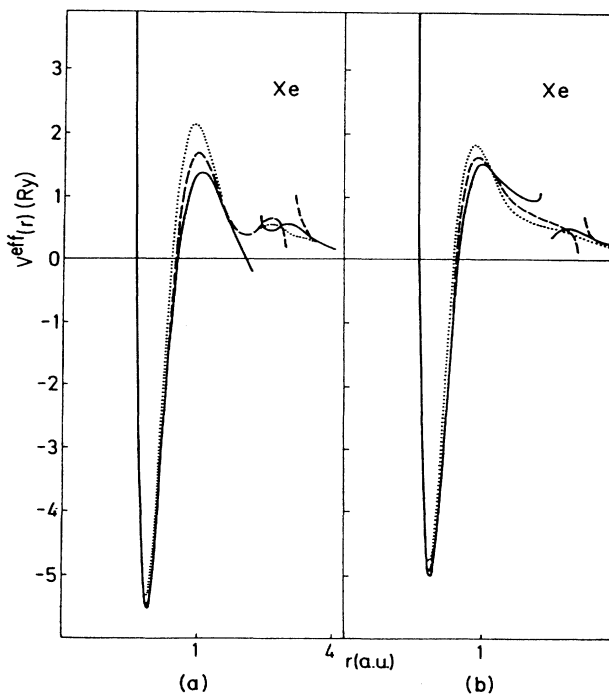


FIG. 6. Energy dependence of the effective local potential in atomic Xe. (a) ($4d \rightarrow \epsilon f$) RPAE, frozen $4d$ hole; (b) ($4d \rightarrow \epsilon f$) HF 1P , frozen hole. Energy ϵ of excited f state: (···) $\epsilon=1$ Ry; (---) $\epsilon=2$ Ry; (—) $\epsilon=3$ Ry.

RPAE wave function will be shifted more into the inner region of the potential, and the overlap with the $4d$ ground-state wave function will be smaller, producing a smaller oscillator strength than the HF 1P wave function.

We have also calculated the photoionization spectra with inclusion of relaxation effects. We have allowed the Xe atom to screen the $4d$ core hole by spherical contraction (monopole relaxation), making the hole potential less attractive. One can see from Fig. 5(a) that the effective potential is less attractive in the RPAE with relaxation of the $4d$ hole than in the RPAE without relaxation. Inclusion of relaxation effects does not much change the shape of the potential: it moves the whole inner part of the potential upwards by about 1 Ry, so that the depth is lowered and the barrier raised. As a consequence the f electrons are prevented from penetrating into the deep hole region until the energy is considerably increased. As a result, the cross section is broadened and its maximum pushed to higher kinetic energy in comparison with the frozen-core RPAE result.

We have also carried out a single-shell ($4d$) RPA calculation based on an LDA basis set. The LDA potential is similar to the HF_{av} potential in what concerns the general shape in the core region. It exhibits a higher barrier than the frozen HF_{av} potential, which is, in our opinion, due to the presence of self-interaction which simulates relaxation (see I). The effect is that outside of the inner-well region, the LDRPA potential is strongly repulsive, more than the RPAE one, as seen in Fig. 5(b).

In Fig. 6 we show the effective one-electron potentials in the HF 1P and the RPAE with a frozen hole for a set of energy values. We see that with increasing energy the barrier decreases, while the bottom of the potential well changes very slightly. The same conclusion is valid for the effective potential in the RPAE with relaxation of the $4d$ hole, apart from the fact that the barrier is higher with respect to the RPAE without relaxation. Examining the LDRPA potentials, we have found the same behavior as in the RPAE with relaxation which accounts for the similar shape of the cross section in these two schemes at higher energies. [The similarity with the cross section obtained in TDLDA (Refs. 24 and 25) indicates that the effective potential for excited states in TDLDA will show the same energy dependence (see I).] Figure 6 shows that while the HF 1P potential is monotonically decreasing in the outer barrier region, apart from the singularities, there is a bump in the RPAE potential in the barrier region at about $r = 2.2$ a.u. This coincides with the barrier that already exists in the HF_{av} potential. In the HF 1P and RPAE potentials, a pronounced peak appears at $r \approx 1$ a.u., i.e., at the position at which the HF_{av} potential has an attractive potential well. These locations correspond roughly to the positions of the maximum amplitude of the $4d$ and $5p$ HF_{av} orbitals. In this way, the HF_{av} potential shows that an excited f electron sees an attractive $4d$ hole at $r \approx 1$ a.u. and feels the repulsion of $5p$ electrons. On the other hand, by inclusion of the polarization via the HF 1P approximation, an excited f electron will feel an additional strongly repulsive interaction with the $4d$ subshell, which is even more pronounced if Fermi-sea correlations are included. Hence, the shell structure of Xe is

mirrored in the effective potential seen by f electrons, through the competition between the electrostatic and the centrifugal contributions. The same effect appears in the effective potential calculated in the RPAE with the relaxed $4d$ hole and in the LDRPA effective potential.

C. Ba, Ba¹⁺, Ba²⁺

The character of the f levels in Ba has attracted much attention in recent years.^{27,30,31,48–51} Basically, the effective potential for the f level in atomic Ba, as well as in Xe, Cs, and La, shows a structured barrier at about $r \approx 1–4$ a.u. and a shallow potential well of Coulombic character $-1/r$ in the outer region. In comparison with Xe, the difference concerns essentially the fact that in Ba, the inner-well–inner-barrier region has been lowered due to the greater nuclear attraction. This will, however, have interesting consequences concerning the localization of f electrons. The wave function and the energy level of the excited state depend on the excitation process, i.e., on the shell from which an electron is promoted to the f level. It is known^{50,51} that the $4f$ wave function, if excited from the $3d$ shell in Cs, Ba, and La, will be localized in the inner potential well. If excited from the $5d$ shell in La,^{32,33} the $4f$ wave function will have a rather diffuse character and will be sitting mainly in the outer shallow potential well. However, the most interesting process is the excitation from the $4d$ shell. This excitation process will involve collective effects leading to a rather complicated situation analyzed in a number of papers.^{11,12,20–25,52} The $4d \rightarrow 4f$ oscillator strength, which carried almost 80% of the oscillator strength in the HF_{av} approximation, was shifted to the continuum in the HF 1P and RPAE. Moreover, as was shown by Wendin,^{13,20} in order to describe satisfactorily the $4d \rightarrow f$ partial photoionization cross section of Ba, the effects of relaxation, as well as the relativistic shift of the binding energy had to be incorporated. In the RPAE with relaxation and relativistic effects, the oscillator strength distribution then agrees quite well with experiment, as shown in Fig. 7. Subsequently, Amusia *et al.*²¹ and Kelly *et al.*²³ have shown that the potential from a statically relaxed ion core combined with the RPAE or MBPT gives good agreement with the experimental photoionization cross section for Ba.

In the following we shall present the general features of the excited state potential for f electrons in atomic Ba and ionized Ba (Ba¹⁺, Ba²⁺). We shall also discuss the dependence of the effective potential on various screening effects. Intra-atomic screening as well as extra-atomic screening (metallic Ba) will be analyzed and their influence on the shape of the excitation cross section will be demonstrated.

Let us begin by discussing the $4d \rightarrow f$ excitation in neutral atomic Ba. An analysis of the effective potential for excited f states in the discrete energy region in the HF_{av} and HF 1P approximations has been given by Wendin and Starace.²⁷ They have shown how the strength of the electrostatic interaction in the 1P channel makes the effective potential seen by HF 1P orbitals much narrower, with a pronounced barrier at $r \approx 1$ a.u., in contrast to the effec-

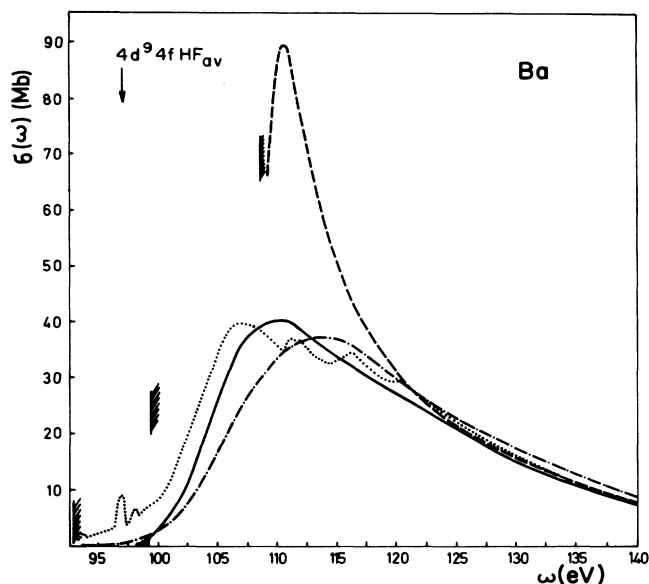


FIG. 7. $4d \rightarrow \epsilon f$ photoionization cross section for atomic Ba: (—) RPAE, with relaxed $4d$ hole; (---) RPAE, with frozen $4d$ hole; (-·-) RPAE, with relaxed $4d$ hole and extra-atomic screening of a $5d$ electron; (····) experimental results according to Rabe *et al.* (Ref. 53). Hatched bars indicate $4d$ ionization energies (metal, atom, frozen HF atom).

tive potential for HF_{av} orbitals. The effect on the photo-absorption cross section is an upwards shift of the $\text{HF}_{\text{av}} 4d \rightarrow 4f$ oscillator strength into the continuum in the $\text{HF } 1P$.

In the presence of a $4d$ hole, the $5d$ orbital becomes localized inside the $6s$ radius, leading to a strong ionic configuration mixing in the $4d$ ionization process. Wending^{12,54} and Connerade *et al.*⁵⁰ found the energy of the $4d^9 5d^2$ configuration in Ba to be lower than the $4d^9 6s^2$ configuration. Physically this means that the creation of a core hole may cause a drastic redistribution of the electronic charge, $6s^2 \rightarrow 5d 6s \rightarrow 5d^2$, in the outermost region of the Ba atom, resulting in a prominent satellite structure in XPS spectra.⁵⁴ Figure 8 shows the changes of the effective potential for an f electron at the kinetic energy $\epsilon = 0.1$ Ry, calculated within the RPAE with a relaxed $4d$ hole, in different ionic configurations. With increasing number x of the $5d$ electrons, $6s^{2-x} 5d^x$, the inner well of the potential is shifted upwards relative to the vacuum zero. This is a consequence of the fact that the $5d$ orbital in the presence of a $4d$ hole is more localized than the $6s$ orbital, thus increasing the screening of the core hole. The shape of the inner well (bottom of the well to the top of the barrier) is almost rigid. Moreover, the energy of the core level follows the bottom of the inner well in response to variations in the electronic configuration, as seen in Table I.

In metallic Ba the ground-state charge density within the unit cell will relax in about the same way as the charge distribution in the neutral atom. In addition to this intra-atomic screening, there will also be the extra-atomic screening by the $6s 5d$ conduction electrons. The

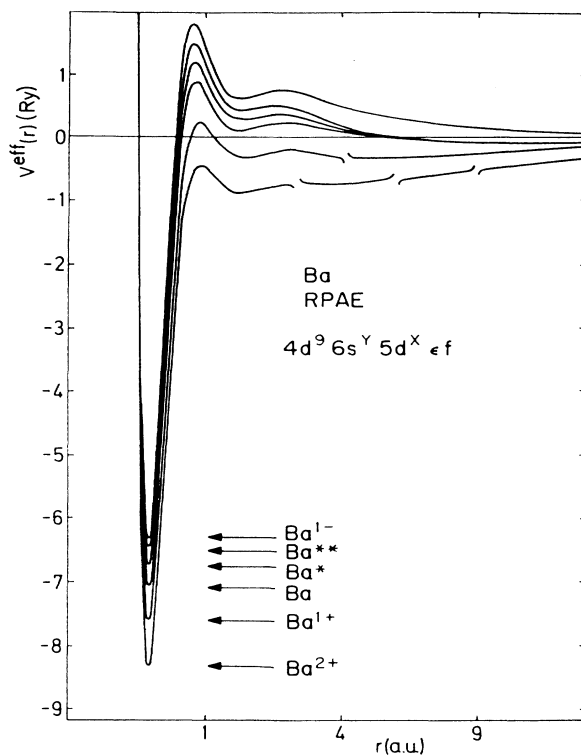


FIG. 8. Effective one-electron local potential ($4d^9 6s^y 5d^x \epsilon f$) RPAE, with relaxed $4d$ hole, in Ba systems for kinetic energy of the excited f state $\epsilon = 0.1$ Ry: Ba^{1-} , with extra-atomic screening of the $5d$ electron, electronic configuration in outermost shells $y=2, x=1$; Ba^{**} denotes configuration with $y=0, x=2$; Ba^* denotes configuration with $y=1, x=1$, Ba denotes $y=2, x=0$; Ba^{1+} denotes ion with configuration with $y=1, x=0$; Ba^{2+} ion, configuration with $y=0, x=0$.

latter process will screen out the long-range part of the core-hole potential neutralizing the hole by adding one unit charge to the unit cell at the site of the core hole. As already mentioned, in the presence of a $4d$ hole in atomic Ba the $5d$ wave function is localized in the inner atomic region, with a maximum at nearly the same place as the $5p$ wave function (at $r \approx 1.9$ a.u.), as shown in Fig. 9. We shall therefore model the screening charge in metallic Ba by a $5d$ orbital. The effect on the HF_{av} potential is shown in Fig. 10. The entire potential is shifted upwards with respect to the potential without extra-atomic screening. We note that *this potential is rather close to the potential for an electron in the absence of the core hole*, indicating that the charge distribution in these two configurations, $4d^9 5s^2 5p^6 5d^1 6s^2 \epsilon f$ and $4d^{10} 5s^2 5p^6 6s^2 \epsilon f$, are quite similar from the point of view of an f electron.

Involving the Hartree form of the effective potential

$$V(\epsilon, r) = - \frac{2[Z - S(\epsilon, r)]}{r}, \quad (3.1)$$

where the electron-electron interaction is represented through an effective screening charge $S(\epsilon, r)$, we can show how the effective shielding of the nuclear field changes in

TABLE I. The monopole relaxation shift Δ_{4d}^M of the $4d$ level for various configurations and ionization stages of Ba. All values are in Ry. V_{\min}^{eff} is the depth of the inner well of the effective potential obtained in RPAE with relaxation effects. To obtain the $4d$ -ionization threshold we have assumed the same relativistic level shift of 0.297 Ry for the center of gravity of the $4d$ shell in Ba^{1+} and Ba^{2+} , as in the neutral Ba.

Final-state configuration	ϵ_{4d}	$\epsilon_{4d}^{\text{HF}}(\Delta\text{SCF})$	Δ_{4d}^M ^a	V_{\min}^{eff}
$4d^9 5s^2 5p^6 5d^1 6s^2$	-8.003	-7.100 ^b	0.903 ^b	-6.44
$4d^9 5s^2 5p^6 5d^2$	-7.771	-7.236	0.535	-6.60
$4d^9 5s^2 5p^6 5d^1 6s^1$	-7.855	-7.385	0.470	-6.80
$4d^9 5s^2 5p^6 6s^2$	-8.003	-7.575	0.427	-7.20
$4d^9 5s^2 5p^6 6s^1$	-8.388	-8.008	0.380	-7.8
$4d^9 5s^2 5p^6$	-8.856	-8.548	0.308	-8.4

^a $\Delta_{4d}^M = \epsilon_{4d}^{\text{HF}}(\Delta\text{SCF}) - \epsilon_{4d}$.

^b The effect of extra-atomic relaxation is included.

different situations. For a free neutral atom $S(\epsilon, r)$ approaches $Z-1$ for large r values, giving the proper Coulomb tail to the effective potential.

In Fig. 11 we show the difference between $S(\epsilon, r)$ calculated for the excited f state with $\epsilon=0.1$ Ry in the RPAE with a relaxed $4d$ hole and a frozen $4d$ hole, without extra-atomic screening. Figure 11 shows clearly the increase in effective shielding of the nuclear field as a consequence of pulling the effective charge into the inner region in a relaxed-hole calculation as compared with a frozen-hole calculation. With the extra-atomic screening of the $5d$ electron, $S(\epsilon, r)$ approaches Z for large r . In Fig. 11 we also show the difference of $S(\epsilon, r)$ calculated in the RPAE with a relaxed $4d$ hole, with and without extra-atomic screening. This figure shows the increase of the shielding of the nuclear field even in the inner potential region, around the $4d$ shell at $r \sim 1$ a.u. In fact the effective nuclear charge is close to zero. The inner well and barrier of the effective potential is raised with respect to the potential without extra-atomic screening. In addition, the shape of the barrier is somewhat changed, influencing

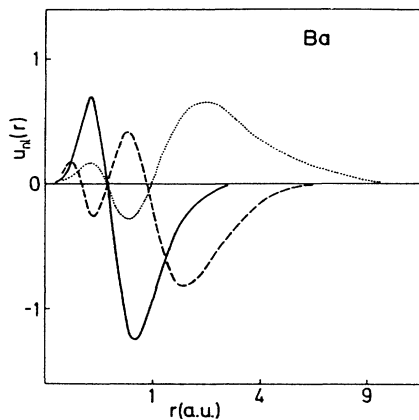


FIG. 9. HF wave functions for atomic Ba: (—) $4d$ ground state; (---) $5p$ ground state; (⋯⋯) $5d$ calculated in the presence of the $4d$ hole.

the detailed shape and position of the cross section. As a result, the $4d \rightarrow f$ photoionization cross section becomes shifted upwards in energy and broadened, as shown in Fig. 7. The $5d$ screened $4d \rightarrow f$ ionization cross section can be compared with the photoabsorption cross section of atomic Ba in Fig. 7. Rabe *et al.*⁵³ have demonstrated experimentally that the atomic and metallic cross sections are practically identical. However, the agreement is clearly poor, and we conclude that the induced charge dis-

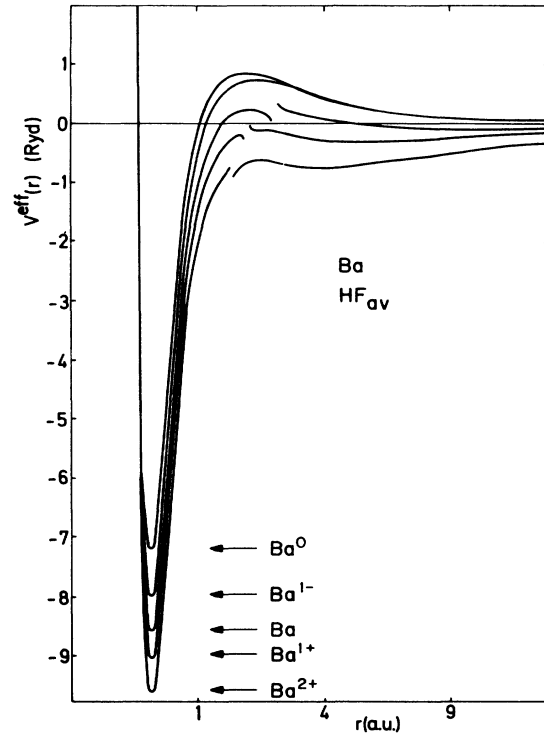


FIG. 10. One-electron local potentials in HF_{av} approximation, Ba systems, $\epsilon=0.1$ Ry: Ba^0 denotes $(4d^{10}6s^25d^0\epsilon f)$ HF potential; for other potentials, with relaxed $4d$ hole, notation is the same as in Fig. 8.

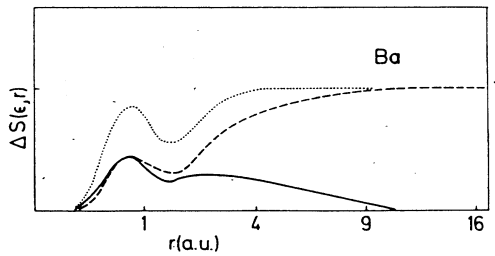


FIG. 11. Difference $\Delta S(\epsilon, r)$ between the effective screening charge $S(\epsilon, r)$ calculated in the RPAE for $\epsilon=0.1$ Ry in atomic Ba: (—) the difference between the screening charge calculated with relaxed and frozen $4d$ hole; (---) the same, calculated with relaxed $4d$ hole with extra-atomic screening of the $5d$ electron and relaxed $4d$ hole, without extra-atomic screening shows the effect of extra screening of the $5d$ electron; (⋯⋯) the sum of the preceding two differences.

placements of the $4d$ shell in the giant dipole resonance region are strongly localized and do not induce extra-atomic relaxation of any importance, in agreement with previous ideas.^{12,13} The f -electron wave packet screens the core hole and prevents long-range relaxation. On the other hand, the excitation is not enough localized to prevent intra-atomic relaxation.

For excitation close to the Fermi level, the f electrons must necessarily leave the ion core in a fully relaxed state including extra-atomic screening, in order to give the correct $4d$ binding energy (see Fig. 7 and Table I). There is then a region above the metallic $4d$ threshold where the extra-atomic screening must become switched off. This is a dynamic problem (papers I and II, and Refs. 10, 13, 20, and 55) which cannot be handled with statically relaxed potentials. The same is, in principle, also true in the purely atomic case.

In summary, the extra-atomic screening of the $4d \rightarrow f$ excitations is not relevant in the giant dipole resonance region. It is, however, relevant for excitations close to the Fermi level and for determining the $4d$ binding energy. The atomic excitation model can also be applied to metallic La as well as to some lanthanides, such as Ce, Gd, Lu, Eu, and Yb, which do not change the configuration and density of f levels upon condensation into solids.⁵⁶

So far we have considered the effective potential for the f electron in the $4d \rightarrow f$ excitation channel in the Ba system, having various configurations in the outmost shells $5d$ and $6s$. We shall now briefly discuss the effective potential for an f electron in Ba^{1+} and Ba^{2+} ions.

As reported by Lucatorto *et al.*,⁵⁷ in Ba^{1+} the continuum resonance still dominates the $4d$ absorption spectrum. The spectrum of Ba^{2+} , on the other hand, shows an entirely different character. Several strong resonances appear in the discrete region, while the absorption cross section decreases monotonically above the $4d$ threshold. The problem has been given considerable attention,⁵⁸⁻⁶² and is quite well understood and reasonably well described.

Figure 8 shows the excited f -state potential ($4d^9\epsilon f$) for $\epsilon=0.1$ Ry in the RPAE. With increasing ionicity, the whole inner part of the effective potential becomes pulled

down by approximately 0.5 Ry in Ba^{1+} with respect to neutral Ba. In Ba^{2+} the potential is again pulled down by about 0.5 Ry with respect to Ba^{1+} . The same also holds in the HF_{av} approximation, Fig. 8. By varying the valence charge distribution, one can therefore monitor the depth of the potential in the inner-well region.⁶³

However, the shape of the inner-well-barrier region is almost rigid because the collective response (induced potential) is localized to the $4d$ shell and is roughly independent of changes in the external environment. Therefore, for small variations of the external screening with respect to neutral Ba, the general shape, the center of gravity, and the width of the $4d-\epsilon f$ oscillator strength distribution will not vary much even though the $4d$ ionization threshold in Ba^{2+} may move up beyond the peak of the average distribution (i.e., the broad peak in neutral Ba, Fig. 7). Since the core levels follow the bottom of the inner well, the position of the giant dipole resonance (or any core transition for that matter, e.g., $3d-4f$) will be quite insensitive to variations in the external screening.⁶⁴

We also note that the effective local potential mirrors the shell structure of Ba. As seen in Fig. 8, the first and second barrier of the RPAE effective potentials are at nearly the same positions where the maximum amplitudes of the $4d$ and $5p$ wave functions appear.

Finally, one could consider the question whether the present results may be utilized in solid-state calculations. The inner-well-barrier region will be nearly the same in the atom and in the corresponding molecule, solid, or adsorbate, and might be used as inner potential in a photoionization calculation which includes the external potential with scattering on the neighboring ions. This might handle photoelectron diffraction effects in giant dipole resonance regions.⁶⁵

IV. SUMMARY

In this paper we have analyzed electronic excitation processes in many-electron atoms in terms of effective local potentials, comparing HF_{av} potentials with HF^1P and RPAE potentials, with and without relaxation effects. We have demonstrated that the collective response of the system shows up through an energy-dependent contribution to the effective potential in the region of space where the responding (core-excited) shell is situated. This leads to a repulsive contribution which narrows the inner well and also leads to a barrier. While in the HF_{av} approximation the effective potential is almost independent of energy over the entire resonance region, in the HF^1P scheme and, in particular, the RPAE there is an important energy dependence for the excitation processes we have considered.

This energy dependence is more pronounced in the region close to threshold, where collective effects (polarization, exchange effects) are more important than at higher energies (clearly demonstrated by a collective barrier that appears in the HF^1P and RPAE local potentials). At sufficiently high kinetic energies the induced polarization potentials of the HF^1P and RPAE represent small perturbations of the HF_{av} potential, the RPAE potential tending to zero faster than the HF^1P one.²

We have also compared the effective local potentials obtained within the RPAE and LDRPA (local-density RPA). Again we note (cf. Ref. 2) that there are great similarities between the effect of self-interaction in the local-density scheme (LDRPA) and relaxation effects in the HF scheme (RPAE).

We have examined the dependence of the effective f -electron local potential for $4d \rightarrow \epsilon f$ excitation processes in Ba on various intra- and extra-atomic screening effects. In particular, we have considered the possibility of modeling $4d$ ionization in metallic Ba by adding an extra-atomic $5d$ screening electron. The resulting $4d \rightarrow \epsilon f$ cross section does not agree well with experiment, however. We conclude that the $4d$ response (induced charge) in the resonance region is so localized that it does not give rise to any extra-atomic relaxation of any importance. Therefore, the atomic excitation model may be used for calculation of giant dipole resonances in metallic Ba, as well as in some lanthanides that do not change configuration and density of f levels upon condensation into solids.⁵⁶ Actually, an atomic model with the configuration of the solid

should always be useful.

However, in molecules and ionic crystals ($\text{BaF}_2, \text{BaCl}_2$; see Ref. 64) and in solids, in general, the scattering of the photoelectron against the neighboring atoms may lead to strong interference effects, and the surrounding potential will then be of great importance. There the effective local excitation potential, which includes atomic polarization and relaxation effects and which is capable of describing giant dipole resonances, might be useful if it can be matched to the surrounding potential.⁶⁵

Finally, we have shown that the change in the ionicity of the system $\text{Ba} \rightarrow \text{Ba}^{2+}$ does not much influence the collective response of the $4d$ shell. Roughly speaking, it moves the inner-well-barrier region down in a rigid manner together with the core levels. As a result, the position and shape of the giant dipole resonance become rather insensitive to outer-shell ionization: When the $4d$ ionization energy increases and discrete structure appears, the giant dipole resonance still determines the distribution of discrete and continuum oscillator strength.

*Present and permanent address: Rudjer Bošković Institute, P.O. Box 1016, 41001 Zagreb, Yugoslavia.

¹Ž. Crljen and G. Wendin, Phys. Scr. **32**, 359 (1985).

²Ž. Crljen and G. Wendin, preceding paper, Phys. Rev. A **35**, 1555 (1987).

³T. M. Zimkina, V. A. Fomichev, S. A. Gribovskii, and I. I. Zhukova, Fiz. Tverd. Tela **9**, 1447 (1967) [Sov. Phys. Solid State **9**, 1128 (1967)].

⁴U. Fano and J. W. Cooper, Rev. Mod. Phys. **40**, 441 (1968).

⁵J. A. R. Samson, in *Handbuch der Physik*, edited by W. Mehlhorn (Springer-Verlag, Berlin, 1982), Vol. 31, p. 123.

⁶A. F. Starace, in *Handbuch der Physik*, edited by W. Mehlhorn (Springer-Verlag, Berlin, 1982), Vol. 31, p. 1.

⁷M. O. Krause, in *Synchrotron Radiation Research*, edited by H. Winnick and S. Doniach (Plenum, New York, 1980), p. 101.

⁸D. M. P. Holland, K. Codling, J. B. West, and G. V. Marr, J. Phys. **12**, 2465 (1979).

⁹F. Gerken, J. Barth, and C. Kunz, in *X-Ray and Atomic Inner-Shell Physics-X82 (International Conference, U. of Oregon, 1982)*, Proceedings of the International Conference on X-Ray and Atomic Inner-Shell Physics, AIP Conf. Proc. No. 94, edited by B. Crasemann (AIP, New York, 1982), p. 602; E. Radtke, J. Phys. B **12**, L77 (1979).

¹⁰G. Wendin, in *New Trends in Atomic Physics*, Les Houches Summer School Session XXXVIII, 1982, edited by G. Grynberg and R. Stora (Elsevier Science Publishers, New York, 1984), p. 555.

¹¹G. Wendin, Phys. Lett. **46A**, 119 (1973).

¹²G. Wendin, in *Vacuum Ultraviolet Radiation Physics*, edited by E. E. Koch, R. Haensel, and C. Kunz (Vieweg/Pergamon, Berlin, 1974), p. 225.

¹³G. Wendin, in *Photoionization and Other Probes of Many-Electron Interactions*, NATO ASI series, edited by F. Wuilleumier (Plenum, New York, 1976), p. 61.

¹⁴E. Radtke, J. Phys. B **12**, L71 (1979).

¹⁵J. W. Cooper, Phys. Rev. Lett. **13**, 762 (1964).

¹⁶S. T. Manson and J. W. Cooper, Phys. Rev. **165**, 126 (1968).

¹⁷M. Ya Amusia, N. A. Cherepkov, and L. V. Chernysheva, Zh. Eksp. Teor. Fiz. **60**, 160 (1971) [Sov. Phys.—JETP **33**, 90

(1971)].

¹⁸G. Wendin, Phys. Lett. **37A**, 445 (1971).

¹⁹G. Wendin, J. Phys. B **6**, 42 (1973).

²⁰G. Wendin, Phys. Lett. **51A**, 291 (1975).

²¹M. Ya. Amusia, V. K. Ivanov, and L. V. Chernysheva, Phys. Lett. **59A**, 191 (1976).

²²M. Ya. Amusia, Appl. Opt. **19**, 4042 (1980).

²³H. P. Kelly, in *Atomic Physics 8*, edited by I. Lindgren, A. Rosén, and S. Svanberg (Plenum, New York, 1982), p. 305.

²⁴A. Zangwill and P. Soven, Phys. Rev. Lett. **45**, 204 (1980); Phys. Rev. A **21**, 1561 (1980).

²⁵A. Zangwill, in *Atomic Physics 8*, edited by I. Lindgren, A. Rosén, and S. Svanberg (Plenum, New York, 1982), p. 339.

²⁶G. Wendin, Phys. Rev. Lett. **53**, 724 (1984).

²⁷G. Wendin and A. F. Starace, J. Phys. B **11**, 4119 (1978).

²⁸The problem of $4f$ localization and two-well potentials was first discussed by Goepfert-Meyer (Ref. 29). For further discussion of these kinds of problems, see J. P. Connerade (Ref. 30), Griffin *et al.* (Refs. 31 and 32), and Band *et al.* (Ref. 33).

²⁹M. Goepfert-Meyer, Phys. Rev. **60**, 184 (1941).

³⁰J. P. Connerade, Contemp. Phys. **19**, 415 (1978); in *New Trends in Atomic Physics*, Les Houches Summer School Session XXXVIII, 1982, edited by G. Grynberg and R. Stora (Elsevier Science Publishers, New York, 1984).

³¹D. C. Griffin and M. S. Pindzola, Comments At. Mol. Phys. **13**, 1 (1983).

³²D. C. Griffin, K. L. Andrew, and R. C. Cowan, Phys. Rev. **177**, 62 (1969).

³³I. M. Band and V. I. Fomichev, Phys. Lett. **75A**, 178 (1980); I. M. Band, V. I. Fomichev, and M. B. Trzhaskovskaya, J. Phys. B **14**, 1103 (1981).

³⁴G. Wendin, in *Photoionization of Atoms and Molecules*, Proceedings of the Daresbury One-Day Meeting, edited by B. D. Buckley, 1978, p. 1; G. Wendin and Ž. Crljen, Bull. Am. Phys. Soc. **24**, 237 (1979).

³⁵Ž. Crljen, Ph.D. thesis, University of Zagreb, 1984.

³⁶D. L. Miller and J. Dow, Phys. Lett. **60A**, 16 (1977).

³⁷D. L. Miller, J. D. Dow, R. G. Houlgate, G. V. Marr, and J.

- B. West, *J. Phys. B* **10**, 3205 (1977).
- ³⁸G. Wendin, *J. Phys. B* **5**, 110 (1972).
- ³⁹J. C. Slater, *Phys. Rev.* **81**, 385 (1951); J. W. Cooper, *ibid.* **128**, 681 (1962); R. M. Sternheimer, *ibid.* **96**, 951 (1954); J. E. Hansen, *J. Phys. B* **5**, 1083 (1972).
- ⁴⁰B. Cadioli, U. Pincelli, E. Tosatti, U. Fano, and J. L. Dehmer, *Chem. Phys. Lett.* **17**, 15 (1972); P. R. Hilton, S. Nordholm, and N. S. Hush, *J. Chem. Phys.* **67**, 5213 (1977).
- ⁴¹L. Hedin and A. Johansson, *J. Phys. B* **2**, 1336 (1969).
- ⁴²G. Wendin and M. Ohno, *Phys. Scr.* **14**, 148 (1976); M. Ohno and G. Wendin, *J. Phys. C* **15**, 1287 (1982).
- ⁴³M. Ya. Amusia and N. A. Cherepkov, *Case Stud. At. Phys.* **5**, 47 (1976).
- ⁴⁴D. J. Kennedy and S. T. Manson, *Phys. Rev. A* **5**, 217 (1972).
- ⁴⁵G. V. Marr and J. B. West, *At. Data Nucl. Data Tables* **18**, 507 (1976).
- ⁴⁶G. Wendin and Ž. Crljen (unpublished).
- ⁴⁷R. Haensel, G. Keitel, and P. Schreiber, *Phys. Rev.* **188**, 1375 (1969).
- ⁴⁸G. Wendin, *J. Phys. B* **9**, L297 (1976).
- ⁴⁹J. E. Hansen, A. W. Fliflet, and H. P. Kelly, *J. Phys. B* **8**, L127 (1975); A. W. Fliflet, H. P. Kelly, and J. E. Hansen, *ibid.* **8**, L268 (1975).
- ⁵⁰J. P. Connerade and M. W. D. Mansfield, *Proc. R. Soc. London, Ser. A* **341**, 267 (1974); **348**, 239 (1975).
- ⁵¹R. C. Karnatak, J. M. Esteve, and J. P. Connerade, *J. Phys. B* **14**, 4747 (1981); B. Sonntag, J. Nogata, J. Sato, Y. Satow, A. Yagishita, and M. Yanagihara, *ibid.* **17**, L55 (1984).
- ⁵²A. W. Fliflet, R. L. Chase, and H. P. Kelly, *J. Phys. B* **7**, L443 (1974).
- ⁵³P. Rabe, K. Radler, and H.-W. Wolff, in *Vacuum Ultraviolet Radiation Physics*, edited by E. E. Koch, R. Haensel, and C. Kunz (Vieweg/Pergamon, Berlin, 1974), p. 247.
- ⁵⁴G. Wendin, *Struct. Bonding (Berlin)* **45**, 1 (1981).
- ⁵⁵G. Wendin, in *X-Ray and Atomic Inner-Shell Physics-X82 (International Conference, U. of Oregon, 1982)*, Proceedings of the International Conference on X-Ray and Atomic Inner-Shell Physics, AIP Conf. Proc. No. 94, edited by B. Crasemann (AIP, New York, 1982), p. 495.
- ⁵⁶B. Johansson and N. Mårtensson, *Phys. Rev. B* **21**, 4427 (1980).
- ⁵⁷T. B. Lucatorto, T. J. McIlrath, J. Sugar, and S. M. Yonger, *Phys. Rev. Lett.* **47**, 1124 (1981).
- ⁵⁸J. P. Connerade and M. W. D. Mansfield, *Phys. Rev. Lett.* **48**, 131 (1982).
- ⁵⁹K. Nuroh, M. J. Stott, and E. Zaremba, *Phys. Rev. Lett.* **49**, 862 (1982).
- ⁶⁰H. P. Kelly, S. L. Carter, and B. E. Norum, *Phys. Rev. A* **25**, 2052 (1982).
- ⁶¹C. Clarke, *J. Opt. Soc. Am. B* **1**, 626 (1984).
- ⁶²Ž. Crljen and G. Wendin (unpublished).
- ⁶³Cf. similar discussion by Connerade, Ref. 30.
- ⁶⁴P. Rabe, Ph.D. thesis, University of Hamburg, 1974.
- ⁶⁵G. Wendin, *Solid State Commun.* **38**, 197 (1981).